Shape Optimization of Rectified Brick Blocks for the Improvement of the out-of-Plane Behavior of Masonry

Dora Foti

Abstract— In this article the numerical and experimental study on different brick blocks for masonry structures or infill walls is developed. The blocks are rectified ones and are shaped in the way to get a better behavior with respect to out-of-plane forces such as the seismic ones. In particular the distribution of the forces in the cross section is defined in function of the shape of the holes. The stress state in the block is investigated by a finite element analysis and the results are compared with the experimental tests carried on individual blocks.

Keywords— Brick blocks, hollow shape, experimental tests, numerical modeling.

I. INTRODUCTION

THIS article addresses the issue of shaping and modeling the brick blocks to improve their behavior with regard to out-of-plane compressive forces. These forces are usually due to wind and earthquake loads; a better behavior of brick masonries to these loads could reduce the possibility of collapse or detachment of masonry panels or infill walls inside reinforced concrete (r.c.) frames.

Masonry structures are subject to horizontal loads that produce a global behavior due to the shear and bending stresses in the plane and a local effect generated by out-of-plane behaviors. Failure in unreinforced masonry buildings due to out-of-plane loads is considered the main cause of personal injury and loss of life during earthquakes [1]. The collapse mechanisms of out-of-plane could be simple or complex (if also the orthogonal wall to the direction of excitation collapses) overturning and bending vertically and horizontally. These four mechanisms can be clearly different for extension, if the collapse interests single walls or connected walls, or only the top parts or entire corners [2], [3].

The possible mechanism depends on the type and quality of the masonry, on its texture and the connecting elements (e.g. tie-rod that increases the box-like behavior) or on the anchorage between structural elements (the node wall-slab) and the type of horizontal elements. The previous

D. Foti is with the Polytechnic of Bari, 70125 Bari, Italy (corresponding author; phone: +39-080-5963771; fax: +39-080-5963719; e-mail: d.foti@poliba.it).

mechanisms of collapse may also occur in the presence of efforts considerably lower than the maximum strength of the walls.

Another parameter to consider is the slenderness of the masonry walls. In this case, in fact, the effect on the walls of orthogonal actions due, for example, to the wind or the forces of inertia related to the earthquake, are significant and produce geometric effects of the second order, considering the negligible tensile strength and deformation deferred over time. In particular, if the roofs of the building are not rigid and, therefore, they are made with deformable systems, the effect of the out-of-plane forces is aggravated by the inability of the structure, as a whole, to redistribute horizontal loads on the resisting walls, such as earthquake and wind.

Today in masonry building manufacturing, the majority of hollow bricks produced are used in two basic applications. The first is in reinforced or unreinforced single-wythe structural walls. Hollow brick units provide both the structural component and the brick finish without the need for additional materials. The compressive and flexural strength of hollow brick masonry depends on unit strength, mortar type, mortar bedding area, grouting and thicknesses of face shells and webs.

More recent research has indicated that the percentage of voids in a brick has no significant effect on the flexural strength of the resulting fully bedded masonry prism [4]. Because sound insulation increases with increasing wall weight, brick masonry provides very good sound penetration resistance. The excellent fire-resistant qualities of brick masonry are well known and together with a very good sound penetration resistance, especially with increasing wall weight.

In order to improve the out-of-plane strength of masonry, in this paper the out-of-plane strength of the brick blocks composing it is studied. It is important to improve the behavior of the blocks in order to improve also the behavior of masonry infill walls interacting with the r.c. frames [5].

The purpose is to understand which areas of the cross section of a brick block accumulate high stresses, i.e. how the stresses distribute inside the section of the individual block. Up to now the numerical models utilized are in fact often applied to the entire masonry to define the behavior of masonry walls [6], [7], [8], [9] or bodies [10] or for modeling

portions or the whole building [11], [12], [13] [14]. At the individual block, modeling studies focus mainly on pairs [15] or are aimed at studying complex dynamics of rigid blocks [16].

Only rarely instead this technique is used for a single block in order to evaluate the mechanical characteristics as a function of the geometry of the septa. The optimized results are easily utilized for different methods of analysis which comply with the code procedure [17].

In this research, it was performed a comparison of different geometries of the cross section of rectified brick blocks, showing the variation of the distribution of stresses at the different shapes of the holes.

The research was developed both experimentally and numerically and is aimed to assess the stress states induced by external actions, such as earthquakes, starting with the management of the geometry of the baffles.

Three different geometries constituting the blocks were thus shaped through the use of finite element codes in the experimental part.

The numerical modeling proposed here followed a phase of experimental characterization of individual blocks to find out the optimized mechanical properties of the brick blocks and to compare the numerical results with the experimental ones.

II. Experimental Assumptions for Implementing the Models

In the present work it was assumed that the brick blocks are all made of the same material; the geometries of the considered blocks correspond to those of some bestselling product currently manufactured by different firms. The aim was to study the role of geometry in the mechanical strength of the blocks in "poroton" material. In particular, reference is made to the following values of the mechanical parameters: modulus of longitudinal elasticity $E = 26068.80$ N/mm^2; Poisson's ratio $\nu = 0.23$.

The first step of this research was to define the behavior of brick blocks to determine the state of stress and deformation of the system subject to loads acting ou-of- plane as a function of its geometry and the condition of the assigned load. Then the behavior is compared to the data obtained from the experimental tests.

The basic assumptions of the modeling can be summarized as follows:
– Septa employed as two-dimensional plate-like elements;
– Absence of internal defects in the material due to the manufacturing process;
– Homogeneous and isotropic material that is modeled as a continuous body with the same constitutive properties in all directions;
– Linear elastic behavior of the material;
– Linear analysis of the model.

It was then rated the criterion of resistance to be set.

A criterion of resistance transforms a state of multi-axial stress in a state of uniaxial stress, ideal or equivalent, that is, with an equal dangerousness of the actual stress state towards the attainment of the limit situation, thereby allowing at evaluate, for the generic point, a maximum ideal stress σi_d^{max} and a minimum ideal stress σ_{id}^{min}.

Among the different existing criteria the one that was used to estimate the ideal stress in the blocks was the Mohr-Coulomb one.

The criterion of Mohr-Coulomb assumes that the collapse of the material occurs when, in a generic point, for a fixed orthogonal force, the absolute value of the shear stress acting on an inclined plane passing through that point, equals the sum of the cohesion c (constant value) and a term proportional to the normal stress acting on the same plane:

$$\tau \leq c - \sigma \, tg\phi \tag{1}$$

where:
σ is the component normal to the stress vector;
τ is the component tangential to the stress vector;
c is the cohesion of the material;
ϕ is the angle of internal friction of the material.

Indicating with σ_{rc} and σ_{rt}, respectively, the compressive and tensile strengths, the following expressions are obtained in function of the parameters c and ϕ.

$$\sigma_{rc} = \frac{2c \cos\phi}{(1 - sen\,\phi)} \tag{2}$$

$$\sigma_{rt} = \frac{2c \cos\phi}{(1 + sen\,\phi)} \tag{3}$$

Applying these expressions and knowing the experimental values of the ultimate compression and tensile strengths of the materials utilized in the numerical analysis, it results:
$c = 11.98$ MPa
$\phi = 38.78°$

III. Modeling of the Brick Blocks

The study on the out-of-plane compressive strength has been conducted, in particular, on three types of poroton bricks for reinforced masonry with vertical holes, which differ substantially for the geometric shape of the holes and have dimensions almost similar.

The basic assumptions are those defined in section II.

The software used for the numerical analysis to model the blocks in finite elements (FE) is STRAUS-7 [18].

The first step was to insert the drawing of the sections of the blocks formed solely by dots, and through some elements called plate, i.e. two-dimensional elements of different

geometry, it was modeled the input design; in particular, among the existing plate elements, quad4 and tri3 plate elements were used.

Subsequently it was made a discretization of the model, i.e. the single plate was divided into an integer number of parts, the same for all the plates, in order to make more precise the results issued by the software.

The block was constrained through hinges on one side and, on the other hand, a compressive unitary force has been applied uniformly over the entire thickness of 19 cm, in the opposite direction compared to the one shown in Fig. 1.

A. Brick Block 1

The first block to be modeled is the one shown in Fig.2. The cross section is made up of rectangular cells and septa with constant dimensions. This geometry is defined as "Brick 1".
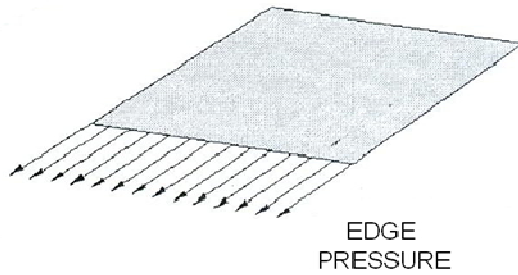
Fig. 1 compressive force in the plane

The first step was to define the mesh of the model and the constraints. A study of the possible constraints of the model was developed to simulate the support of the block in the testing equipment. The characterization of the material and the definition of the "plate element propriety" were derived from the experimental tests conducted at the Official Laboratory for Material Testing "M. Salvati" of the Polytechnic of Bari, and summarized in Table 1, with an out-of-plane compressive strength equal to 2.0 N/mm^2.
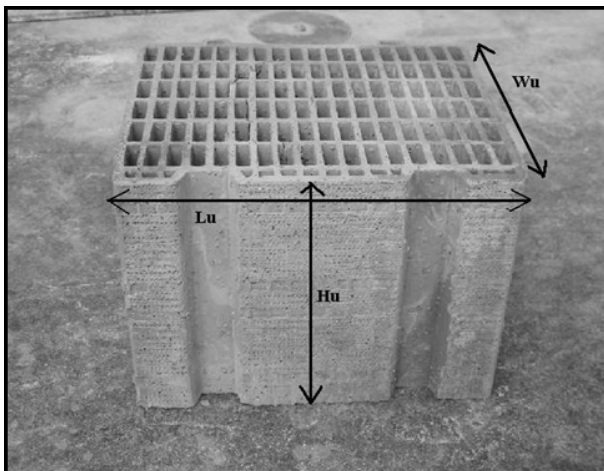

Fig. 2 alveolater block

Hinge-like constraints have been hypothesized to allow a free rotation of the nodes at the ends of the block; fix nodes have been assumed for the side of the block in contact to the testing equipment.

A very dense mesh has been considered in the modeling, to get a better discretization of the problem. The model, in fact, was made up of a number of 4,048 nodes and 3,690 plates (Fig. 3).

The load condition in the out-of-plane direction of the masonry was subsequently set. Fig. 4 shows the distribution of the principal stresses σ_{11} and σ_{22}. In the figure the darker areas represent the higher stressed parts of the cross section of the brick.

As it is possible to notice, the distribution of the maximum stresses precisely occurs in the vertical baffles that make up the bricks and experimentally proved to be the first parts to crack (Fig. 4). Moreover, the failure mechanisms are similar to those that occurred experimentally, i.e. with the damage and crack of the internal baffles.

Table 1 material characteristics and properties of "Brick 1" obtained from the tests

| Total area	74717.7 mm^2
Net area = (Total area)*(100-%voids)	35012.71 mm^2
Percentage of voids	47.89 %
Ultimate compressive load	1407 kN
Compressive strength of the brick material σ_{rc}	15 N/mm^2
Tensile strength of the brick material σ_{rt}	9.23 N/mm^2
Longitudinal elastic modulus	E_t = 24711.96 N/mm^2
Poisson's coefficient = v	0.23
"Out-of-plane" ultimate load of the block	134.33 kN
"Out-of-plane" compressive strength of the block	2.0 N/mm^2
"In-plane" compressive strength of the block	4.21 N/mm^2
c	11.98 MPa
ϕ	38.78°
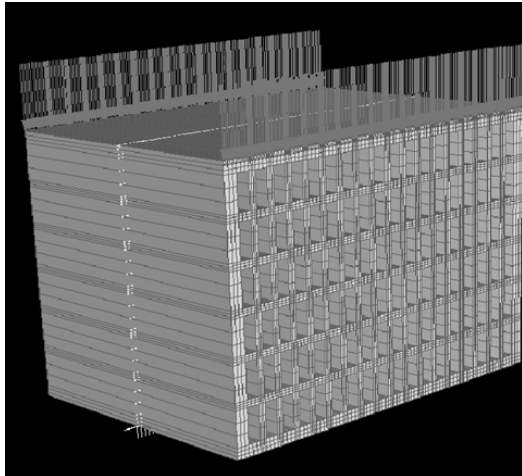
Fig. 3 three-dimensional model of the block.

To evaluate the load at failure of the entire system the crack in the considered point has been assessed and thus the ideal compressive stresses, σ_{idc}, are evaluated. Appling the criterion of Mohr-Coulomb the maximum ideal compressive strength is obtained from the modeling. The maximum ideal compressive stresses, σ_{idc}^{MAX}, were directly obtained from the computer aided numerical analysis. The criterion used for their calculation is the Mohr-Coulomb one, obtaining σ_{idc}^{MAX} equal to 8.50 N/mm^2 inside the septa.
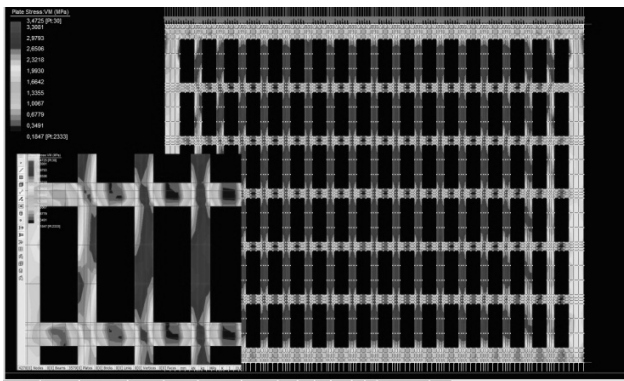

Fig.4 distribution of the stresses in the brick block

Knowing the experimental compressive strength of the brick material, σ_{rc}=15 N/mm^2, the ultimate strength was calculated multiplying the applied unit load for K, multiplier of the limit condition equal to the ratio $\sigma_{rc}/\sigma_{idc}^{MAX}$, which allows the occurrence of the failure condition in the most severely stressed point of the system.

The ultimate failure stress σ_Y equal to 1.70 N/mm^2 was then obtained:

$$K = \frac{\sigma_{rc}}{\sigma_{idc}^{Max}} = 1.70$$

$$\sigma_Y = K \cdot 1N/mm^2 = 1.70\ N/mm^2$$

It is observed then as the value of the load at failure, defined through numerical analysis, is slightly lower than the experimentally declared value, obtaining anyway a value more than acceptable, considering all the simplifications made in the model.

B. Brick Block 2

Other types of geometries for the septa and the cells of the brick were subsequently modeled. A further block was then modeled, characterized by a geometry constituted by rectangular cells and 2 gripping holes suitable for reinforced masonry, called "Brick 2" (Fig.5).
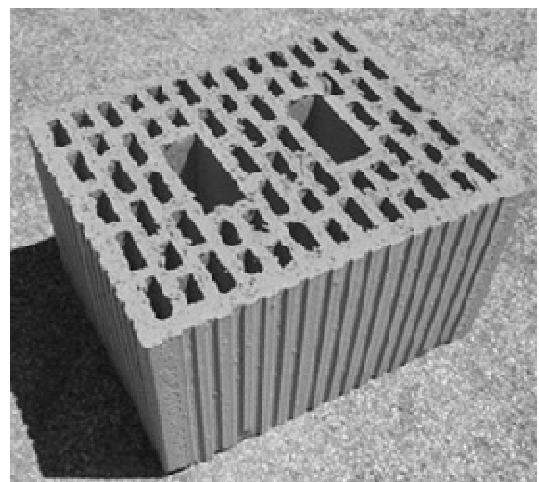

Fig. 5 geometrical scheme of Brick 2

Also in this case a series of experimental tests have been performed to evaluate the mechanical characteristics of the brick block. Their values are summarized in Table 2.

Table 2. Material properties and mechanical characteristics of "Brick 2" obtained from the tests

Total area	75000 mm^2
Percentage of voids	45 %
Minimum thickness of the extreme septa	10 mm
Minimum thickness of the septa	7.2 mm
Compressive strength of the brick material σ_{rc}	15 N/mm^2
Tensile strength of the brick material σ_{rt}	9.23 N/mm^2
Longitudinal elastic modulus	24700 N/mm^2
Poisson's coefficient = ν	0.23
"Out-of-plane" compressive strength of the block	3.80 N/mm^2

The mesh has then been defined (Fig. 6), utilizing 29,395 nodes and 27,300 plates, obtaining a total of 57,952equations.

The maximum ideal stress σ_{idc}^{MAX} equal to 5.58 N/mm^2 has been then obtained. The maximum values of the stress were obtained around the gripping holes (Fig.7).

Appling the criterion of Mohr Coulomb the results obtained from the numerical analysis are very close to those obtained experimentally, with a value of the multiplier K equal to 2.68 and an ultimate failure stress σ_Y equal to 2.68 N/mm^2.

Comparing this block to Brick 1, it is observed a reduction of the mechanical performance of the block.
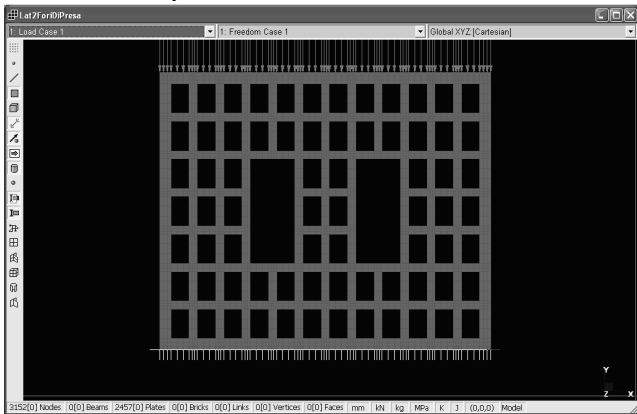

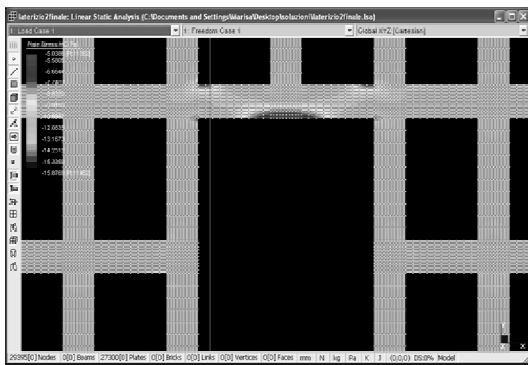Fig.6 geometrical and loading definition of the model for Brick 2

Fig.7 areas of stresses concentration for Brick 2

C. Brick Block 3

It was subsequently modeled a block with a single central gripping hole (Brick 3). It presents a percentage of voids equal to 45%; they are rectangular holes with an area of 450 mm^2. The single gripping hole is larger than the other rectangular holes, with an area of 3,450 mm^2 (Fig. 8).
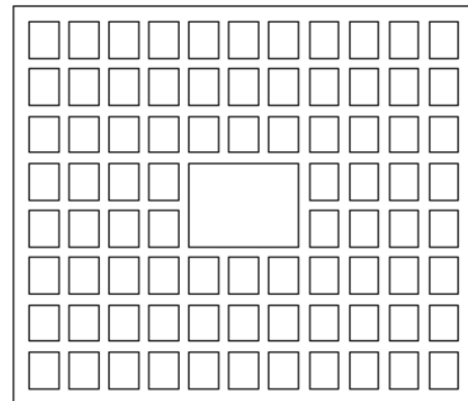

Fig.8 geometrical scheme of Brick 3

The characteristics obtained from the experimental tests for Brick 3 are shown in Table 3.

.

Table 3. material properties and mechanical characteristics of Brick 3 obtained from the tests

Total area	75000 mm^2
Percentage of voids	45 %
Minimum thickness of the extreme septa	10 mm
Minimum thickness of the septa	7.2 mm
Compressive strength of the brick material σ_{rc}	15 N/mm^2
Tensile strength of the brick material σ_{rt}	9.23 N/mm^2
Longitudinal elastic modulus	24700 N/mm^2
Poisson's coefficient = ν	0.23
"Out-of-plane" compressive strength of the block	2.50 N/mm^2

The finite element modeling was then implemented leading to a mesh composed of 31,525 nodes and 29,400 plates. Solving a system of 62,414 equations it has been determined a maximum ideal stress, σ_{idc}^{MAX}, equal to 6.03 N/mm^2.

Even in this case the higher stresses were concentrated in the neighborhood of the gripping hole that, even in this geometry, is the most sensitive point (Fig. 9) with an ultimate failure stress σ_Y equal to 2.48 N/mm^2.
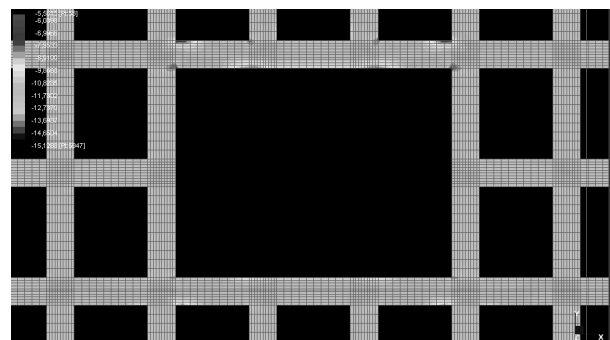
Fig. 9 concentration areas of the stresses in Brick 3

IV. RESULTS

From the data obtained it can be concluded that in general the areas with the maximum values of the stresses are located near the grip holes for all the geometries of the blocks tested. In detail for each individual case, it is possible to notice some small differences.

Observing the block indicated as "Brick 2", having the rectangular holes and provided with two gripping holes, it is well evident to find that globally the stress state affecting it is low and it is represented by light grey with lighter spots. However, a more precise analysis reveals the presence of areas in which the stress reaches a peak value. These areas are localized in the vicinity of the grip holes, in the central area of the upper side. It is enough to consider only one intake hole because the stress distribution is the same for both. Observing well the image it is possible to notice other two high stress small areas that are located practically at the foot of the two holes overlying the gripping hole, i.e. in the upper part of the horizontal partition that precedes it.

Analyzing the image in Fig. 10, which presents the development of stresses along the lower side of the gripping hole, it can be seen that the areas in darker grey, indicating the values of the maximum stresses, have an extension reduced compared to those present in the upper part but are located practically in the same positions; in fact, if we imagine a horizontal axis which divide the block into two parts, the positions of the areas in darker grey would be symmetrical albeit of a different extension.

So it is possible to say that, moving away from the loading floor, the possibility that high values of the stresses that could trigger the collapse of the block occurred, is undoubtedly decreased.
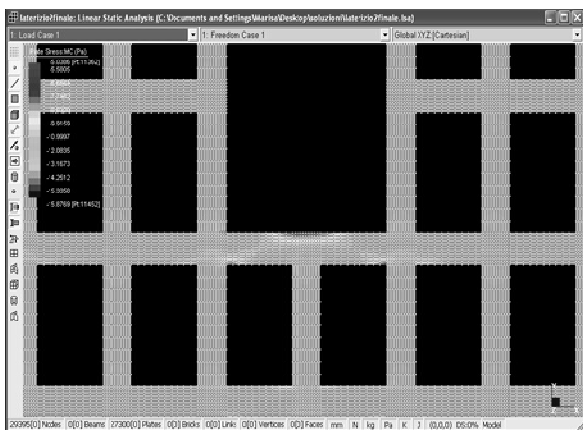

Fig. 10 distribution of stresses in the lower part of Brick 2

It is possible to notice that in both horizontal and vertical baffles, or both in the orthogonal ones and in those parallel to the loading direction, the values of the stresses are low to medium regardless of their distance from the top; therefore the medium stress distribution is independent of the distance from the loading floor.

At the sides of the gripping hole for Brick 2, similarly to Brick 1, neither maximum nor minimum values occur (see Figs. 7 and 10).

In fact the values of the stresses are low to medium, irrespective of their distance from the upper side and are always colored in light grey in Fig. 10; therefore, the distribution of the medium stress is independent of the distance from the loading floor. As already stated before, the higher stresses are positioned around the gripping holes.

The same considerations can be drawn for Brick 3, while in the case of Brick 1 the highest stresses are uniformly distributed in the individual folders making up the cells. It is just possible to notice a general reduction of the average stress state around the holes. At the cross of the vertical and horizontal baffles the stress state increases.

The stress distribution in Brick 3 around the only gripping hole is similar to Brick 2. In the corners, in fact, areas with a very low stress state are visible, while along the upper edge it is possible to notice two areas having higher stresses. It can be said that the stress distribution for the whole block is symmetrical with respect to an imaginary vertical axis able to divide into two equal parts the brick.

From a careful observation it is possible to notice that in the upper part of the block that is between the intake hole and the loading floor, there are areas with both peak stresses and minimum stresses concentrated in the corners of the holes; the peculiarity consists in a perfect alternation of these areas as shown in Fig. 11.
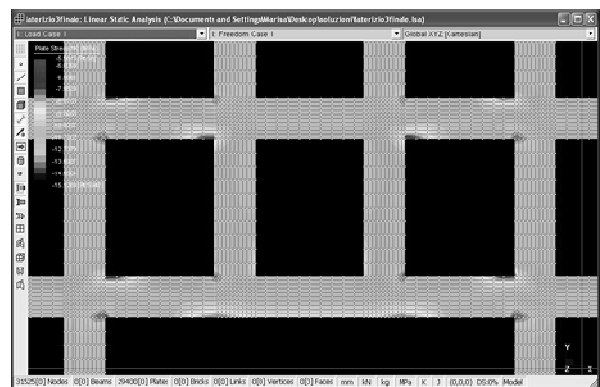

Fig. 11 distribution of stresses in the upper part around the gripping hole of Brick 3.

Summarizing the considerations made for each block, it can be put in evidence that the distribution of stresses presents some important affinity between the three blocks: for each of them it was found that the stress state is medium and uniform along of the cross sections that is, the stress value

appears to be independent of the distance from the loading floor but only closely linked to the size of the load.

Another common feature for all the bricks is the absence of both peak stresses and minimum stresses along those sides of the gripping holes having the same direction of the load that appears as vertical in the figures.

The area around the gripping holes constitutes an exception with respect to the remaining areas interested, precisely, by a common trend, and presents some peculiarity that differs according to the block considered, although, even in this case, it is possible to detect similarities between Brick 2 and Brick 3, which, moreover, have a very different geometry. In fact, while for the last two blocks the areas affected by maximum stresses are concentrated in the central part of the upper corners, for Brick 1, with a very different geometry, the higher stressed area is located along the vertical baffles.

A common feature between the blocks is constituted by the behavior of the stresses along the lower side of the gripping hole that appears to mimic that of the upper part, with regard to the positioning of the peak regions, but stresses appear to have generally lower entities.

Exclusively Brick 3 in the part of the block between the gripping hole and the loading plane shows some singular points, not negligible and discordant respect to the average, affected by high values of stresses, as previously described in detail.

After analyzing in detail the stress distribution in the cross sections of the blocks, a comparison between the numerical and experimental values has been implemented, finding a good correspondence.

The value of the characteristic compressive strength in the orthogonal direction, i.e. perpendicular to the surface of a masonry wall built with Brick 1 type blocks, is equal to 2.0 N/mm^2, while applying the criterion of Mohr-Coulomb it goes on to a value of the ultimate stress slightly lower, equal to 1.70 N/mm^2.

For Brick 2, similarly, it happened that the value of the ultimate stress reached with the criterion of Mohr-Coulomb, is equal to 2.68 N/mm^2 against the value of 3.80 N/mm^2 obtained from the laboratory tests.

For the third and last brick (Brick 3) the ultimate stress obtained from the calculus, equal to 2.48 N/mm^2, is almost equal to the experimental compressive strength equal to 2.50 N/mm^2. Table 3 shows the values of the compressive strength obtained from the numerical analysis and the experimental tests on the blocks.

Table 3 comparison between the numerical and experimental compressive strengths obtained for each block.

Typology	Compressive strength [N/mm²]	
	Numerical	Experimental
Brick 1	1.70	2.00
Brick 2	2.68	3.80
Brick 3	2.48	2.50

To get results more objective and independent of the characteristics of the individual blocks, which obviously derive from the manufacturing of individual construction companies, it was split the values of the ultimate stresses for the weight of the corresponding brick. The weights depend on the percentages of the holes and the geometrical dimensions and, therefore, are slightly different, as shown in Table 4.

Table 4 weights of the tested blocks

Block	Weight (N)
Brick 1	115.0
Brick 2	126.8
Brick 3	84.6

The values of these ratios have been gathered in another histogram shown in Fig.12.
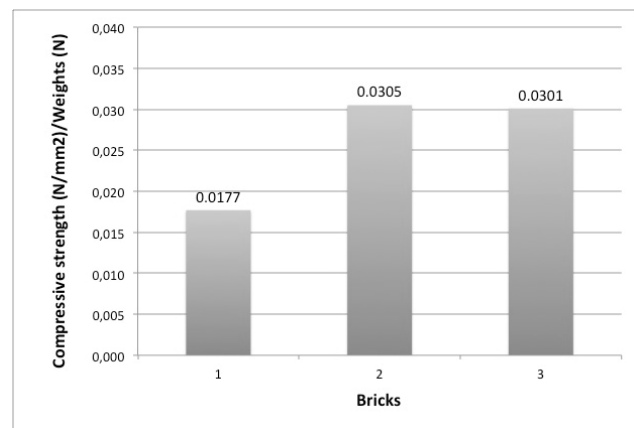

Fig. 12 values of the ratios between the failure stress and the weight for each tested block

The highest value is reached for the Brick 2; therefore, this block has the best performance because in terms of equal weight it can withstand higher stresses before reaching the failure.

V. CONCLUSIONS

This study is part of a larger research project aimed at the evaluation of the mechanical properties of rectified brick blocks; it is also aimed to better define the geometry of the cells. The purpose is to suggest the use of models to simplify the problem and also to evaluate the characteristics of strength of the material.

The present paper had as object the modeling of the brick blocks in order to study the results under out-of-plane

compressive forces. We had gone from a technical description of the blocks tested and had led to the understanding of the stress distribution within them.

As a conclusion the geometry is therefore defined not only in function of the insulating and sound-absorbing characteristics expected from the masonry, leaving to experimental tests the evaluation of the mechanical characteristics, but also in function of the strength characteristics already considered in the design phase.

REFERENCES

[1] M. Indirli, L.A. Kouris, A. Formisano, R.P. Borg, F.M. Mazzolani, "Seismic damage assessment of unreinforced masonry structures after the Abruzzo 2009 earthquake: the case study of the historical centres of L'Aquila and Castelvecchio Subequo". *Int J of Architectural Heritage, Conservation, Analysis and Restoration*, vol. 7, Issue 5, Taylor&Francis Eds, 2012, pp. 536-578.

[2] J.L. Varela-Rivera, D. Navarrete-Macias, L.E. Fernandez-Baqueiro, E.I. Moreno, "Out-of-plane behaviour of confined masonry walls", *Eng Struct*,vol.33, pp.1734-1741,2011. doi:10.1016/j.engstruct.2011.02.012.

[3] G. Milani, M. Pizzolato, A. Tralli, "Simple numerical model with second order effects for out-of-plane loaded masonry walls", *Eng Struct*, vol.48, pp. 98-120, 2013. http://dx.doi.org/10.1016/j.engstruct.2012.08.029.

[4] J.P. Sanders, D.A. Brosnan, "The effect of void area on brick masonry performance", *J of ASTM Int*, vol. 4, Issue 1, ASTM International, West Conshohocken , PA, 2007.

[5] D. Foti, "Influence of infill walls on the seismic behavior of r.c. frames", *Eng Struct*, submitted for publication.

[6] A. Mebarki, Q.H. Bui, R.A. Saada, P. Delmotte, S.S. Tizapa, "A simplified mechanical model to assess the bearing capacity of masonry walls: Theory and experimental validation", *Constr and Build Materials*, vol.23, No.2, 2009, pp. 1109-1117.

[7] C. Sandoval, P. Roca, E. Bernat, E. Gil, "Testing and numerical modelling of buckling failure of masonry walls, *Constr and Build Materials*, Vol.25, No.12, 2011, pp. 4394-4402.

[8] D. Foti, M. Diaferio, N.I. Giannoccaro, M. Mongelli: "Ambient Vibration Testing, Dynamic Identification and Model Updating of a Historic Tower", *NDT&E International*, vol. 47, pp. 88-95, 2012. ISSN:0963-8695, doi:10.1016/ j.ndteint.2011.11.009.

[9] D. Foti, S. Ivorra, M F Sabbà: "Dynamic Investigation of an Ancient Bell Tower with Operational Modal Analysis", *The Open Construction and Building Technology Journal*, vol. 6, pp.384-391, 2012. ISSN 1874-8368, DOI 10.2174/1874836801206010384.

[10] A. Baratta, O. Corbi, "On Variational Approaches in NRT Continua", *Int J of Solids and Struct*, Elsevier Science, Vol.42, pp. 5307-5321, 2005. ISSN: 0020-7683. DOI:10.1016/j.ijsolstr.2005.03.075.

[11] A. Romanazzi, F. Paparella, "Ambiente Urbano: Dissesti Strutturali da demolizione-ricostruzione: Un caso di studio reale", *Structural/L'Edilizia*, Vol.167, 2011 (*in Italian*).

[12] A. Baratta, O. Corbi, "On the equilibrium and admissibility coupling in NT vaults of general shape", *Int J Solids and Structures*, Vol.47, No.17, pp. 2276-2284, 2010. ISSN: 0020-7683. DOI: 10.1016/j.ijsolstr.2010.02.024.

[13] A. Baratta, O. Corbi, "An approach to masonry structural analysis by the no-tension assumption—Part II: load singularities, numerical implementation and applications". *Applied Mechanics Reviews*, vol. 63, no. 4, pp. 040803-1/21, 2010. ISSN: 0003-6900, DOI:10.1115/1.4002791.

[14] D. Foti: "On the numerical and experimental strengthening assessment of tufa masonry with FRP", *Mech of Adv Mat and Struct*, vol. 20, Issue: 02, 2013, pp. 163-175, ISSN: 1537-6532, doi: 10.1080/15376494.2012.743634.

[15] W.A. Thanoon, A.H. Alwathaf, J. Noorzaei, M.S. Jaafar, M.R. Abdulkadir, "Nonlinear finite element analysis of grouted and ungrouted hollow interlocking mortarless block masonry system", *Eng Struct*, vol.30, no.6, pp. 1560-1572, 2008.

[16] A. Baratta, O. Corbi, "Analysis of the dynamics of rigid blocks using the theory of distributions", *J of Adv in Eng Software*, vol.44, no.1, pp.15-25, 2012. ISSN: 09659978, DOI: 10.1016/j.advengsoft.2011.07.008.

[17] D. Foti, M. Debernardis, V. Paparella, "Structural Safety Control of Masonry Buildings: Non-Linear Static Seismic Analysis with a Non-Linear Shear Strength Criterion". In: B.H.V. Topping, (Editor), *Proceedings of the Eleventh International Conference on Computational Structures Technology*. Civil-Comp Proceedings, Stirlingshire: Civil-Comp Press, ISBN: 978-1-905088-54-6, ISSN: 1759-3433, Dubrovnik, 4-7 sept. 2012, doi: 10.4203/ccp.99.

[18] STRAUS 7, v 2.3.3, Strand7 Pty Ltd (AUS).